Investigation of parameter-free model polarization potentials for electron-molecule scattering calculations including the nuclear motion

Michael A. Morrison and Bidhan C. Saha
Department of Physics and Astronomy, University of Oklahoma, Norman, Oklahoma 73019
(Received 3 March 1986; revised manuscript received 4 June 1986)

A correlation-polarization potential originally introduced by O'Connell and Lane [Phys. Rev. A **27**, 1893 (1983)] is used in e-H_2 scattering calculations in which the vibrational motion of the target is taken into account. Eigenphase sums (as a function of internuclear separation) and cross sections for elastic scattering and for rovibrational excitations are compared to their counterparts calculated using the *ab initio* nonadiabatic model polarization potential of Gibson and Morrison [Phys. Rev. A **29**, 2497 (1984)]. At low energies, these scattering quantities are found to be quite sensitive to the treatment of polarization. To assess these model potentials, theoretical total, momentum transfer, and rotational- and vibrational-excitation cross sections are compared to experimental data.

I. INTRODUCTION

Physicists studying electron-molecule scattering have long known of the importance of polarization effects in low-energy collisions.[1,2] The term *polarization* is something of a catchall, including effects that are of second (and higher) order in the electron-molecule interaction. In a rigorous quantum-mechanical formulation of the collision, polarization manifests itself as virtual excitations of (closed) electronic states of the target.[3]

In spite of impressive progress during the past two decades on exact and approximate methods for including polarization effects in electron-atom and electron-molecule collision theories,[1,4–14] only recently have rigorous treatments (within the rigid-rotator approximation[1]) become computationally feasible.[10–14] Nevertheless, there remains a need for simple, reliable model polarization potentials for calculation of accurate cross sections for electron scattering from complicated molecules, clusters, and surfaces—and for vibrational excitation.

One such model potential—the *correlation-polarization* (CP) *potential*—was introduced in 1983 by O'Connell and Lane,[15] who applied it to electron scattering from rare-gas atoms with phenomenal success. Subsequently there have appeared reports of successful application of CP potentials to electron scattering from an impressive array of molecules[16,17] *in the rigid-rotator approximation.* As this approximation does not allow for the vibrational motion of the target, the next step in exploring this model seemed clear: try it for vibrational excitation.

In this paper we report an implementation of a CP potential to electron scattering from H_2, with special emphasis on vibrational excitation. We compare a variety of scattering quantities—eigenphase sums and integrated and differential cross sections—to their counterparts as determined in calculations using a second model, the *ab initio* nonadiabatic polarization potential of Gibson and Morrison.[7] We also compare various low-energy cross sections to available experimental data. By these comparisons, we elucidate the sensitivity of these scattering quantities to the treatment of polarization.

In Sec. II, we briefly review polarization effects and the problems they pose for the study of vibrational excitation. In Sec. III, we discuss the implementation of the CP potential for vibrational excitation. Then, in Sec. IV, we bring on the results: differential and integrated cross sections for excitation of H_2 from the initial ground vibrational state, $v_0=0$, to $v=1$ and $v=2$.

II. BACKGROUND: POLARIZATION AND ITS DIFFICULTIES

Polarization effects are simplest in the asymptotic region (i.e., at large values of the radial coordinate r_e of the scattering electron) where the polarization potential assumes the *asymptotic form* (AF) (Ref. 1)

$$V_{\rm pol}^{\rm AF}(\mathbf{r}_e,R)=-\frac{\alpha_0(R)}{2r_e^4}-\frac{\alpha_2(R)}{2r_e^4}P_2(\cos\theta_e),\quad r_e\to\infty\ . \qquad (1)$$

In Eq. (1), $\alpha_0(R)$ and $\alpha_2(R)$ are the spherical and nonspherical polarizabilities of the target at internuclear separation R, and the azimuthal angle θ_e is measured from the internuclear axis. Between the asymptotic region and the molecular charge cloud, polarization can still be treated adiabatically—although not by so simple a form as Eq. (1).[4,5] But nearer to the target *nonadiabatic* (i.e., velocity-dependent) polarization effects become important. These dynamic effects give rise to an energy-dependent term in the polarization potential; the importance of this term for low-energy electron-molecule collisions remains unknown.[18] Finally, inside the charge cloud the independent-particle model, which is implicit in Eq. (1) and in adiabatic treatments of polarization, is no longer appropriate, and bound-free correlation must be taken into account.

For many years, polarization effects were represented[1] by including in the electron-molecule interaction potential $V_{\rm int}(\mathbf{r}_e,R)$ a local, energy-independent, heuristic term that was defined by the simple (if drastic) expedient of multiplying Eq. (1) by a *spherically symmetric* cutoff function.

This function depends on a parameter that is usually chosen either by adjusting theoretical cross sections to experimental data[19] or by a physically motivated guess.[20]

At the other theoretical extreme are formulations, such as those based on optical-potential theory[11,12] or pseudostates,[10] in which dynamic polarization effects are treated in an "essentially exact" fashion. All such studies reported to date have been carried out in the *rigid-rotator approximation,* in which the internuclear separation of the target was held fixed throughout the scattering calculation. So the results of these studies do not incorporate the vibrational motion of the target and, of course, exclude vibrational-excitation cross sections.

Between these extremes—neither as crude as a cutoff asymptotic form nor as rigorous as, say, an optical-potential treatment—are theories based on a model polarization potential.[6–9,15–17] The ideal of such a potential would be a local, parameter-free function of $\mathbf{r}_e$ that could simply be added to the static potential in the Schrödinger equation. One such model has been implemented by Gibson and Morrison.[7] Based on a variational treatment of the polarized and unpolarized target[6] near the Hartree-Fock level of accuracy, this model invokes its major approximation in the treatment of nonadiabatic effects, which are incorporated via a nonpenetrating approximation originally introduced by Temkin for electron-atom scattering in the polarized orbital method.[9,21] According to this rather *ad hoc* prescription, the two-electron, bound-free Coulomb interactions are simply "switched off" whenever the projectile coordinate r_e is less than the radial coordinate in the one-particle density function of the target. The resulting model polarization potential is parameter-free, local, and energy independent. To date it has been applied to e-H_2 scattering calculations of differential and integrated elastic,[22,23] rotational- (Ref. 22) and vibrational-excitation[23] cross sections, and to electron-N_2 scattering[24] calculations of the total cross section in the rigid-rotator approximation. Because this potential incorporates effects beyond a purely adiabatic treatment, Gibson and Morrison christened it the BTA ("better than adiabatic") model. These authors further found that for e-H_2 collisions, only the *dipole* term in this potential need be retained; this led them to introduce the "better than adiabatic dipole" (BTAD) potential that is used in the present study.

Although the BTAD scheme does not inflict the computational demands of, say, optical-potential theory, neither is it trivial to calculate. At each internuclear separation, one must perform extensive variational calculations and numerically evaluate large numbers of finite integrals. So for electron scattering from complicated, highly nonspherical molecules—to say nothing of scattering from clusters or surfaces—there is still a need for a simple analytic model polarization potential. Moreover, even for scattering from comparatively simple molecules, a parameter-free model polarization potential would be of great value in the study of vibrational excitation;[25,26] an electron's ability to vibrationally excite a molecule depends critically on the variation of $V_{\rm int}(\mathbf{r}_e,R)$ with R, so regardless of the method used to solve the scattering equations, the R dependence of the polarization potential is crucial. The central problem in devising such a potential is how to continue the asymptotic form (1) into the short-range region in a physically reasonable, parameter-free way. Fortunately, one can tolerate a certain looseness in the model, because near and within the target electrostatic and exchange effects dominate the scattering process.

The CP potential introduced by O'Connell and Lane[15] seems ideal for vibrational-excitation calculations. As we will see in the next section, this potential is quite easy to calculate, for it depends only on the target charge density and the polarizabilities $\alpha_0(R)$ and $\alpha_2(R)$. And, like the BTAD potential, its theoretical foundation is more sound than that of the cutoff asymptotic form, and it is unsullied by parameters that require adjustment to experimental data.

III. THE CORRELATION-POLARIZATION POTENTIAL AND ITS IMPLEMENTATION FOR VIBRATIONAL EXCITATION

The functional form of the CP potential in the problematical short-range region is given by an approximate, local correlation potential energy that is calculated for various ranges of the target probability density $\rho(\mathbf{r},R)$. At each R, we use the form of the correlation potential recommended by Padial and Norcross.[16,27] This potential is expressed in terms of the "density variable" r_s,

$$r_s(\mathbf{r}_e,R)\equiv\left[\frac{3}{4\pi\rho(\mathbf{r}_e,R)}\right]^{1/3}, \tag{2}$$

and, in atomic units (hartrees), is given by

$$V_{\rm co}(\mathbf{r}_e,R)=\begin{cases}0.0311\ln r_s-0.0584+0.00133 r_s\ln r_s-0.0084 r_s, & r_s<1\\ \dfrac{\gamma(1+\frac{7}{6}\beta_1 r_s^{1/2}+\frac{4}{3}\beta_2 r_s)}{(1+\beta_1 r_s^{1/2}+\beta_2 r_s)^2}, & r_s\geq 1\ .\end{cases} \tag{3}$$

The constants in this equation are $\gamma=-0.1423$, $\beta_1=1.0529$, and $\beta_2=0.3334$. These constants do not depend on R. The dependence of this potential on the internuclear separation is carried by the density variable of Eq. (2). Note that since r_s depends on the target probability density ρ, it depends on r_e and θ_e. So, like the other components of the electron-molecule interaction potential, $V_{\rm co}(\mathbf{r}_e,R)$ must be expanded in Legendre polynomials; we use standard computer codes to effect this expansion.[28] From this expansion we obtain the coefficients $v_\lambda^{\rm co}(r_e,R)$

shown in Fig. 1, which are discussed below.

The correlation potential energy in Eq. (3) takes no account of target distortion and so is inappropriate outside the target electron cloud. Happily, each expansion coefficient $v_\lambda^{\rm co}(r_e,R)$ for $\lambda=0$ and 2 crosses the corresponding asymptotic coefficient

$$v_\lambda^{\rm asym}(r_e,R)=-\frac{\alpha_\lambda(R)}{2r_e^4},\quad \lambda=0,2\ . \tag{4}$$

The CP potential $V_{\rm pol}^{\rm CP}(\mathbf{r}_e,R)$ is constructed by the simple (if somewhat *ad hoc*) expedient of "joining" the expansion coefficients $v_\lambda^{\rm co}(r_e,R)$ and $v_\lambda^{\rm asym}(r_e,R)$ for $\lambda=0$ and 2 at r_c^λ—the value of r_e where they cross,[29] i.e.,

$$v_\lambda^{\rm CP}(r_e,R)=\begin{cases} v_\lambda^{\rm co}(r_e,R), & r_e\le r_c^\lambda, \\ v_\lambda^{\rm asym}(r_e,R), & r_e>r_c^\lambda \end{cases} \quad \lambda=0,2\ . \tag{5}$$

In this model, only the spherical and $P_2(\cos\theta_e)$ terms of the polarization potential are retained. Equation (5) provides the desired prescription for continuing $v_\lambda^{\rm asym}(r_e,R)$ inward to the origin without introducing parameters that require adjustment to experimental cross sections. In Fig. 1, the coefficients $v_\lambda^{\rm co}(r_e,R)$ for e-H_2 at equilibrium ($R=1.4a_0$) are compared to the asymptotic expansion coefficients (4) and to coefficients for a purely adiabatic polarization potential[4] and the BTAD potential.

When the target vibrates, the joining radius and the value of the correlation potential at this radius depend on the internuclear separation R. For the e-H_2 CP potential, these quantities are given in Table I for internuclear separations ranging from $0.5a_0$ to $2.6a_0$. (This range more than encompasses the extent in R of the lowest three vibrational wave functions, which is roughly from $1.0a_0$ to $2.0a_0$.) The variations of $r_c^\lambda(R)$ and $v_\lambda^{\rm CP}(r_c^\lambda,R)$ with R are not pronounced—as R increases there is a gradual increase in the former and little change in the latter—but neither are they negligible.

And now we introduce some computational details. The permanent and induced moments of H_2, which are given in Table I, and the charge densities of the target were evaluated from near-Hartree-Fock calculations of

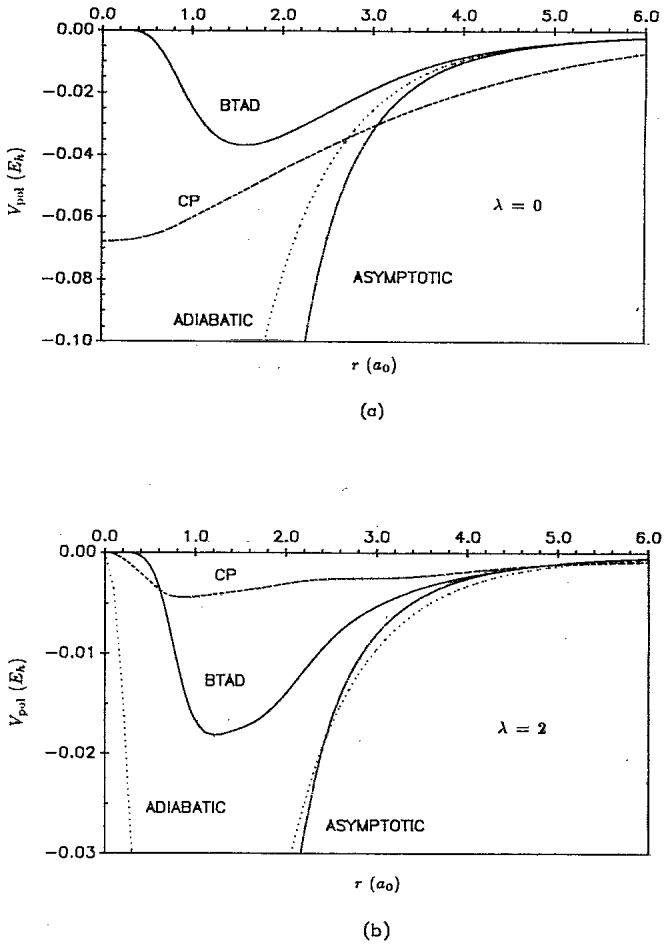

FIG. 1. (a) Spherical ($\lambda=0$) and (b) nonspherical ($\lambda=2$) expansion coefficients of four e-H_2 polarization potentials at $R_{\rm eq}=1.4a_0$. The BTAD (solid curve) and CO (dashed curves) potentials are described in the text, as is the asymptotic potential (dot-dashed curve). The purely adiabatic potential (dotted curve) was calculated variationally with the scattering electron fixed at radial coordinate (Ref. 4).

TABLE I. Molecular moments of H_2 and parameters for calculation of the CP potential for e-H_2 scattering at internuclear separations R. The potential $v_\lambda^{\rm CP}(r_c^\lambda,R)$ is the value of the λth Legendre projection of the potential $V_{\rm pol}^{\rm CP}(\mathbf{r}_e,R)$ at the joining radius $r_c^\lambda(R)$. (1.0[−2]=1.0×10^{-2}.)

R (a_0)	α_0 (a_0^3)	α_2 (a_0^3)	q ($e\,a_0^2$)	r_c^0 (a_0)	$-v_0^{\rm CP}(r_c^0,R)$ (E_h)	r_c^2 (a_0)	$-v_2^{\rm CP}(r_c^2,R)$ (E_h)
0.50	2.047	0.130	0.033	2.3166	3.5543[−2]	3.1350	6.7186[−4]
0.80	2.850	0.319	0.151	2.5500	3.3703[−2]	3.8206	7.4810[−4]
1.00	3.519	0.540	0.244	2.7138	3.2440[−2]	4.1680	8.9448[−4]
1.20	4.302	0.869	0.345	2.8812	3.1212[−2]	4.5503	1.0139[−3]
1.40	5.194	1.305	0.452	3.0481	3.0080[−2]	4.7876	1.2423[−3]
1.60	6.188	1.850	0.564	3.2120	2.9067[−2]	4.9407	1.5526[−3]
1.80	7.315	2.603	0.680	3.3782	2.8084[−2]	5.1274	1.8828[−3]
2.00	8.529	3.426	0.798	3.5376	2.7231[−2]	5.2249	2.2983[−3]
2.20	9.869	4.469	0.916	3.6976	2.6397[−2]	5.3463	2.7349[−3]
2.50	12.083	6.389	1.089	3.9351	2.5196[−2]	5.5167	3.4491[−3]
2.60	12.875	7.130	1.145	4.0140	2.4797[−2]	5.5712	3.7004[−3]

the electronic wave functions of H_2 (using the POLYATOM computer program[30]) at the 11 values of R shown in Table I. The basis set used in these computations was a $[5s\,2p/3s\,2p]$ set of nucleus-centered contracted Cartesian-Gaussian functions. The exponents and contraction coefficients for this basis set were taken from the work of Huzinaga.[31] To determine the BTAD polarization potential and the target polarizabilities we augmented this basis with diffuse Gaussians chosen to realistically accommodate distortions of the target. The resulting $[6s\,3p/4s\,3p]$ basis is given in Table I of Ref. 7. This basis set was used for all values of R—i.e., the variation of the $X^1\Sigma_g^+$ electronic H_2 wave function with internuclear separation was carried solely by the linear variational parameters in the Hartree-Fock calculations. A detailed examination of the resulting electronic energy curve and of various molecular properties will be relegated to a forthcoming paper.[32]

Figure 1 reveals differences in the BTAD and CP potentials at one geometry, equilibrium. More important to vibrational excitation are the matrix elements of this potential between initial and final target vibrational wave functions $\phi_{v_0}(R)$ and $\phi_v(R)$. In Fig. 2 we compare BTAD and CP matrix elements $\langle \phi_{v_0}(R) \,|\, v_\lambda^{\rm pol}(r_e,R) \,|\, \phi_v(R) \rangle$ for

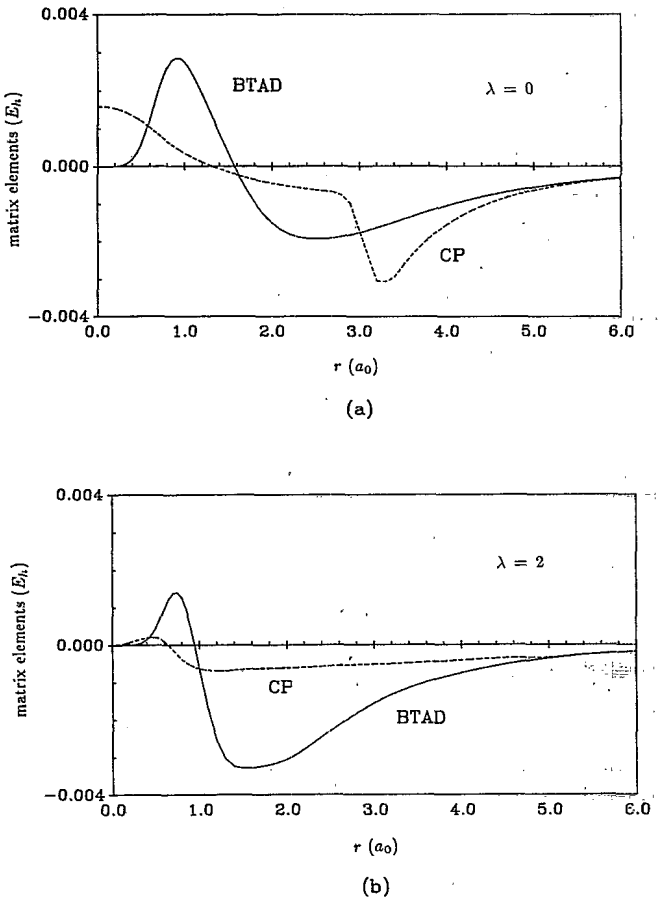

FIG. 2. Coupling matrix elements for vibrational states $v_0=0$ and $v=1$ of the (a) spherical ($\lambda=0$) and (b) nonspherical ($\lambda=2$) Legendre projections of the BTAD (solid curves) and CP (dashed curves) model polarization potentials.

$v_0=0$ and $v=1$. (The vibrational wave functions used in this study were obtained by numerically solving the nuclear Schrödinger equation for the electronic energy curve that was obtained in the aforementioned structure calculations.)

The spherical matrix elements of Fig. 2(a) are primarily responsible for pure vibrational excitation ($v_0=0$, $j_0=0\rightarrow v=1$, $j=0$), and the nonspherical elements of Fig. 2(b) for rovibrational excitation ($v_0=0$, $j_0=0\rightarrow v=1$, $j=2$). In both cases, the BTAD and CP potentials yield strikingly different matrix elements. In the near-target region, however, the static potential is much stronger than the polarization potential. Nevertheless, as we will see in the next section, the differences on display in Fig. 2 significantly affect the vibrational-excitation cross sections.

IV. CROSS SECTIONS: THEORETICAL METHODOLOGY, RESULTS, AND DISCUSSION

Our primary goal is to compare vibrational-excitation cross sections calculated with the CP and BTAD potentials and thereby to explore the sensitivity of these cross sections to the treatment of polarization. But it is also useful to consider briefly elastic scattering and pure rotational excitation; although these scattering processes entail no change in vibrational state, their cross sections are significantly affected by the nuclear motion. Following a description of our scattering calculations, we will examine each of these cross sections in turn.

A. Scattering calculations

We have calculated elastic, pure rotational, pure vibrational, and rovibrational cross sections, using slightly different theoretical prescriptions for elastic and inelastic processes. A rationale for this scheme and details of the calculations themselves—methodology, convergence criteria, and parameters, etc.—will appear elsewhere,[32] but the few remarks in this section will provide a context for the results to follow.

Our computational schemes for elastic and inelastic scattering differ in their treatments of exchange effects and of the dynamical interaction between the electron and the nuclei. *Elastic* cross sections are calculated using the adiabatic-nuclei (AN) method[33] from fixed-nuclei scattering matrices that incorporate exchange effects exactly.[34] But *inelastic* cross sections are calculated using the laboratory-frame close-coupling (LFCC) method[35] with an approximate exchange potential.[36]

One would prefer, of course, to treat exchange (and all other aspects of the scattering problem) exactly, and doing so is feasible for elastic scattering, because accurate elastic cross sections can be calculated using the AN theory.[22,23] Unfortunately, for the e-H_2 system, the AN approximation fails for low-energy inelastic scattering[22] and is especially poor for vibrational excitation.[23] So for these processes, the scattering theory used must incorporate a more accurate representation of the interplay of the nuclear dynamics and the quantum motion of the projectile. In the present study, we fulfill this requirement by implementing the full rovibrational LFCC theory. The price

one pays for the accuracy of the LFCC theory's treatment of the nuclear dynamics is computer time. To mitigate somewhat the computational demands of our LFCC calculations, we approximate the nonlocal exchange operator in the Schrödinger equation by a local, energy-dependent model potential, thereby transforming the coupled *integro-differential* scattering equations of LFCC theory into coupled *differential* equations.

Our model exchange potential is based on a free-electron-gas (FEG) approximation of the target.[36] In the present study this potential has been designed explicitly for the study of inelastic scattering in the following way. For e-H_2 scattering at energies below several eV, inelastic cross sections are dominated by p-wave S-matrix elements (e.g., in the LFCC theory by matrix elements $S^J_{vjl,v_0j_0l_0}$ with $l=l_0=1$). Our FEG exchange potential contains a "tuning parameter" that is chosen at each R so that the eigenphase sum from body-frame *static-model-exchange* calculation reproduces its counterpart from a *static-exact-exchange* calculation. This "tuning" is done at one energy only (0.54 eV) in the Σ_u electron-H_2 symmetry, which is dominated by p waves. It is in this sense that the resulting tuned free-electron-gas exchange (TFEGE) potential is optimized for inelastic scattering.

We have not numerically enforced orthogonality of the scattering function to bound molecular orbitals. Earlier studies of e-H_2 scattering in the rigid-rotator approximation[37] showed the effects of imposing this condition to be minimal when a *tuned* FEG potential is used. The importance of orthogonalization when such a potential is used in calculations of vibrational-excitation cross sections, however, remains to be investigated.

We converged all integrated cross sections and eigenphase sums to better than 1% and all differential cross sections to better than 5% at all angles. To attain this level of convergence, we included in the LFCC expansion basis four vibrational manifolds ($v=0$, 1, 2, and 3); within each vibrational manifold, we included five rotational states, using spherical harmonics for the rotational target functions. We carried out studies of the CP and BTAD potentials for both even- and odd-parity rotational states; but our findings turned out to be independent of the parity of the rotational states, so here we will report results only for the even-j case.

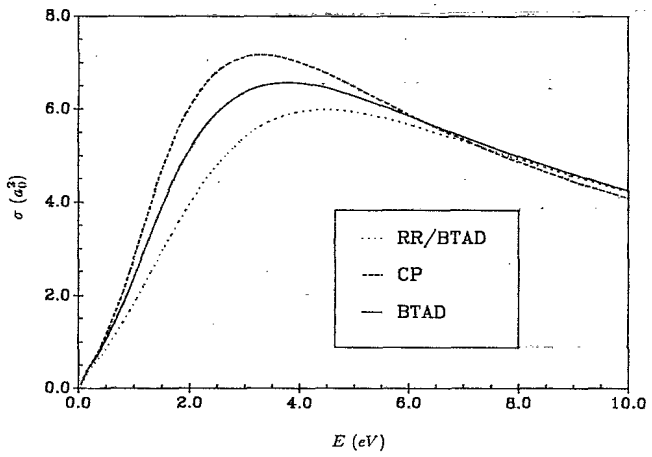

FIG. 3. Elastic-scattering e-H_2 cross sections (from initial state $v_0=0$, $j_0=0$) from AN calculations with the BTAD (solid curve) and CP (dashed curve) potentials. The exchange interaction was treated exactly in these calculations. Also shown are cross sections from a comparable rigid-rotator calculation (RR) (dotted curve) using the BTAD potential at $R=1.4a_0$.

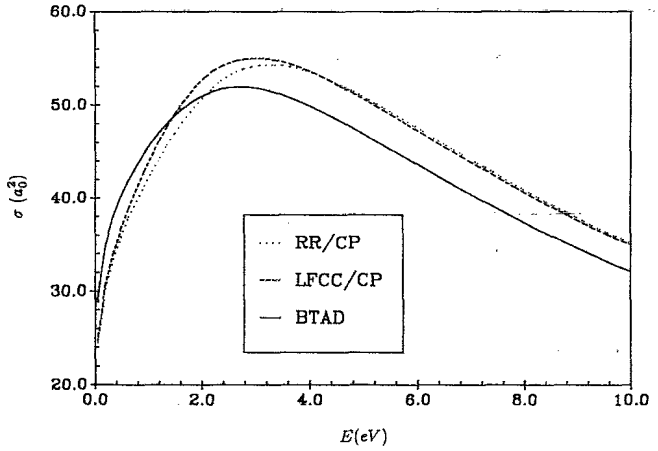

FIG. 4. Integrated LFCC cross sections for the 0,0→0,2 pure rotational excitation of H_2 as determined using the BTAD (solid curve) and CP (dashed curve) polarization potentials. Also shown are rigid-rotator cross sections (dotted curve) using the BTAD potential at equilibrium.

In the comparisons that follow, the computations that produced the BTAD and CP results are identical in every respect except for their treatment of polarization. A few total and rotational-excitation cross sections calculated in the rigid-rotator approximation will also be shown, so that the effects of the vibrational motion of the target on these scattering quantities can be assessed.[11]

B. Elastic cross sections

In Fig. 3 and Table II we compare integrated elastic e-H_2 cross sections calculated using the AN method with

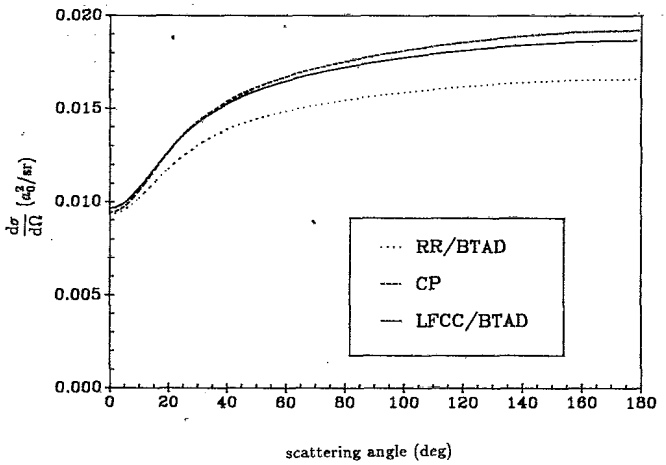

FIG. 5. The differential cross section for the 0,0→0,2 pure rotational excitation at 0.08 eV from BTAD (solid curve), CP (dashed curve), and rigid-rotator (dotted curve) calculations. See caption to Fig. 4 for details.

TABLE II. Electron-H_2 cross sections (in a_0^2) at selected energies (in eV) calculated with the BTAD and CP polarization potentials. The elastic cross sections were calculated using the ANV method with an exact treatment of exchange; the inelastic using LFCC with the Σ_u-tuned FEG exchange potential described in Sec. III. For each energy, the top line gives the BTAD cross sections, the bottom line the CP results.

	$\sigma(a_0^2)$					
Energy (eV)	00→00	00→02	00→10	00→12	00→20	00→22
0.08	30.650	0.214				
	26.340	0.218				
0.20	35.001	0.442				
	30.758	0.467				
0.70	42.754	1.458	0.055	0.026		
	39.938	1.717	0.061	0.032		
1.00	45.519	2.263	0.181	0.137		
	43.883	2.769	0.232	0.181		
1.50	48.898	3.701	0.453	0.453	0.006	0.011
	49.143	4.648	0.623	0.631	0.010	0.019
2.50	51.785	5.659	0.756	0.943	0.047	0.081
	54.503	6.807	0.942	1.177	0.072	0.120
3.00	51.708	6.086	0.748	0.978	0.055	0.088
	55.006	7.126	0.889	1.157	0.074	0.114
3.50	50.974	6.266	0.705	0.952	0.053	0.081
	54.589	7.151	0.807	1.081	0.066	0.095
4.50	48.391	6.187	0.586	0.822	0.043	0.061
	52.200	6.760	0.630	0.870	0.050	0.066
6.00	43.547	5.639	0.425	0.604	0.031	0.040
	47.196	5.890	0.433	0.597	0.033	0.040
8.00	37.322	4.820	0.289	0.400	0.020	0.025
	40.559	4.857	0.286	0.379	0.020	0.023
10.0	32.068	4.129	0.210	0.276	0.014	0.016
	34.903	4.087	0.207	0.259	0.013	0.014

the BTAD and CP polarization potentials. Also shown in Fig. 3 are results from a rigid-rotator calculation in which the internuclear separation was fixed at its equilibrium value of $1.4a_0$. For this system, the CP elastic cross sections are in reasonable agreement with the BTAD results; the percentage difference between them is 10% or less from 0.047 to 10.0 eV, the difference being largest below about 2.0 eV.[38] The error introduced into this cross section by making the rigid-rotator approximation is as great as 5% at energies below 2.0 eV.

C. Pure rotational excitation

In Fig. 4 and Table II we show cross sections for the pure (i.e., vibrationally elastic) rotational excitation 0,0→0,2. As in the elastic case, for this excitation the CP and BTAD cross sections agree reasonably well from threshold (0.044 eV) to 10.0 eV; the agreement is especially good at energies below 0.5 eV. The difference between the integrated CP and BTAD cross sections rises with increasing energy to 26% at 1.5 eV, then decreases.

The differential cross section for this excitation at 0.08 eV is shown in Fig. 5. At this energy (and at others below about 1.0 eV) both model potentials produce a cross section with the same shape. At higher energies the CP and BTAD differential cross sections exhibit larger differences, but these are differences of scale, not of shape. As illustrated in Fig. 5, the rigid-rotator approximation consistently produces integrated and differential cross sections for rotational excitation of H_2 that differ substantially from those obtained when the vibration of the nuclei is taken into account.

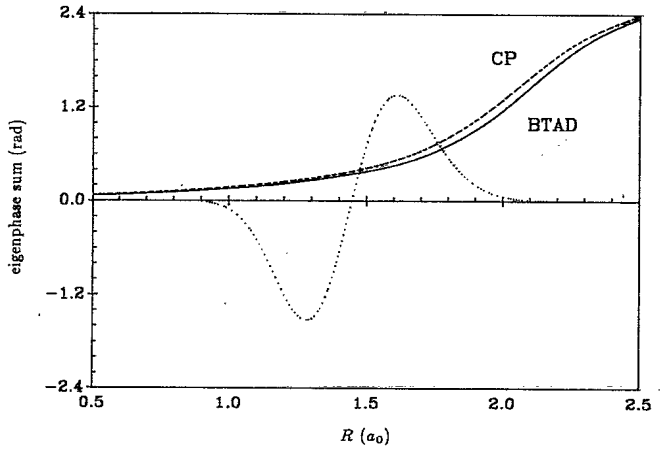

FIG. 6. Eigenphase sums at 1.5 eV in the Σ_u e-H_2 symmetry from body-frame, fixed-nuclei scattering calculations using the BTAD (solid curve) and CP (dashed curve) polarization potentials. Also shown is the product $\phi_0(R)\phi_1(R)$ (dotted curve).

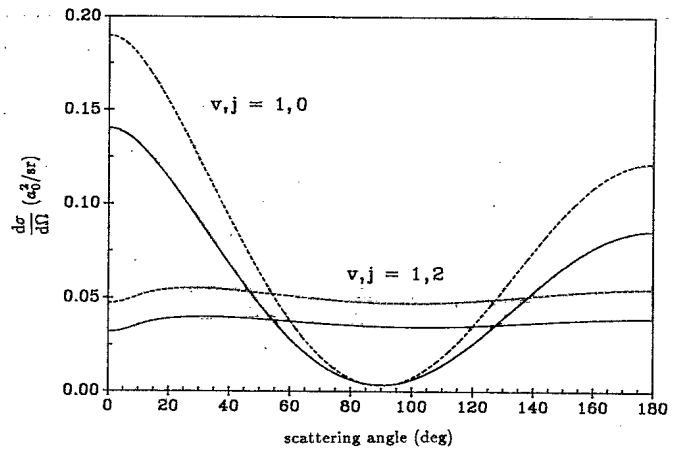

FIG. 8. Differential cross sections at 1.5 eV for the 0,0→1,0 and 0,0→1,2 excitations of H_2 from LFCC calculations using the BTAD (solid curve) and CP (dashed curve) potentials. See Fig. 7 for the corresponding integrated cross sections.

D. Vibrational excitation

We now come to the primary focus of this study: vibrational excitation. Some insight into this scattering process can be gained by examining the variation with R of eigenphase sums for the most important electron-molecule symmetries. The eigenphase sum of interest for inelastic scattering below about 5.0 eV is that of the Σ_u symmetry, because at these energies contributions from this symmetry dominate rotational and vibrational excitation.[39]

In Fig. 6 and Table III are shown the eigenphase sums at 1.5 eV in the Σ_u symmetry as a function of R. (In

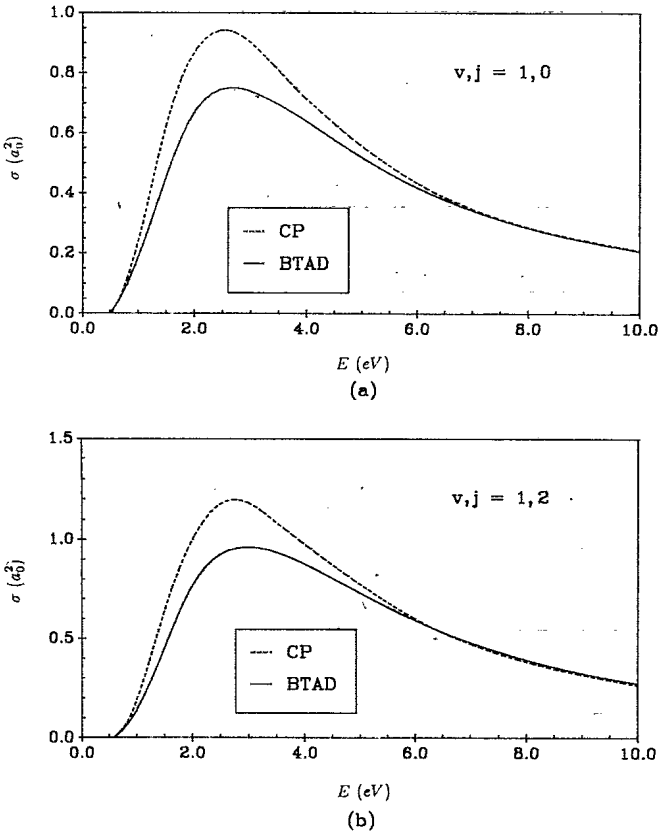

FIG. 7. Integrated vibrational-excitation cross sections for the (a) 0,0→1,0 and (b) 0,0→1,2 excitations obtained from LFCC calculations using the BTAD (solid curve) and CP (dashed curve) polarization potentials.

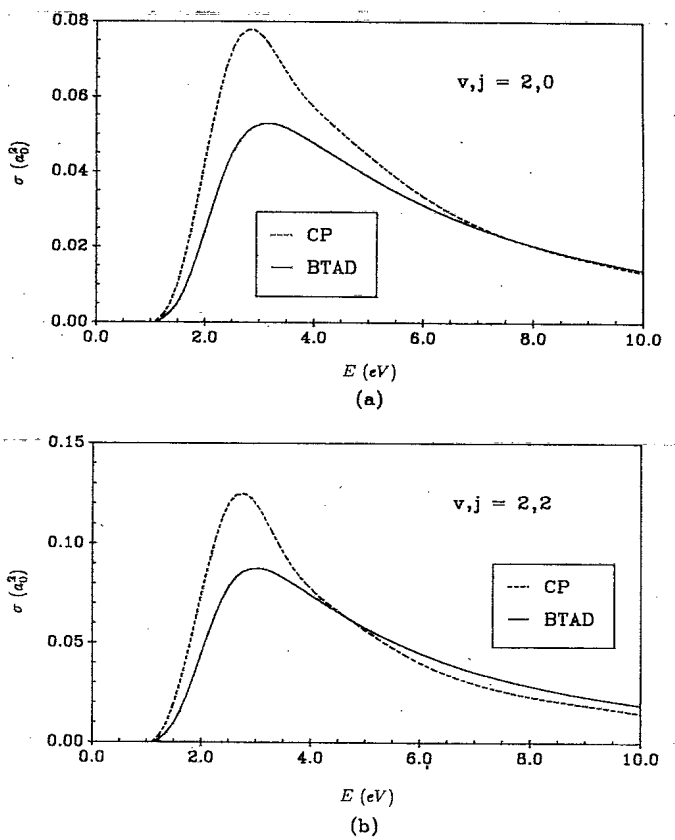

FIG. 9. Cross sections for the (a) 0,0→2,0 and (b) 0,0→2,2 excitations of H_2 from LFCC calculations in which the BTAD (solid curve) and CP (dashed curve) polarization potentials were used.

Table III these data are given at other energies and for the Σ_g and Π_u symmetries; using this table, one can examine the sensitivity of these scattering quantities to polarization as R and E change.) The R variation of the Σ_u CP and BTAD eigenphase sum are quite similar. Yet, the slopes of these eigenphase sums in the critical range of R from $1.0a_0$ to $2.0a_0$—as indicated by the product of vibrational wave functions $\phi_0(R)\,\phi_1(R)$ (the dotted curve in Fig. 6)—are different enough that the AN cross sections from the two models differ considerably. To illustrate this point, we present in Table IV pure vibrational and rovibrational cross sections calculated making the AN approximation for vibration [adiabatic-nuclei vibration (ANV)]. We shall return to this table in the discussion of Sec. IV E.

Because of the inadequacy of the ANV method for low-energy e-H_2 excitations,[23] we resort to the LFCC method. Integrated LFCC cross sections for pure vibrational and rovibrational excitation to the $v=1$ manifold are shown in Fig. 7 and Table II. At energies above 4.0 eV, the CP and BTAD cross sections $\sigma(0,0\rightarrow1,0)$ and $\sigma(0,0\rightarrow1,2)$ agree fairly well. At lower energies, however, the differences between the two are significant. The

TABLE III. Electron-H_2 eigenphase sums (in radians) at selected energies (in eV) and internuclear separations (in a_0) from body-frame fixed-nuclei calculations using the BTAD (upper) and CP (lower) polarization potentials. In these calculations, exchange was treated exactly, using the iterative static-exchange method of Collins *et al* (Ref. 34). (A more complete table of eigenphase sums, including 11 internuclear separations, more energies, and four symmetries, is available on request from the authors.) ($1.0[-2]=1.0\times10^{-2}$.)

E (eV)	Eigenphase sums (rad)				
$R(a_0)$	0.08	0.70	1.0	3.0	10.0
		Σ_g			
1.000	3.030	2.781	2.706	2.392	1.918
	3.038	2.801	2.730	2.430	1.983
1.200	3.028	2.768	2.690	2.366	1.887
	3.036	2.790	2.716	2.407	1.958
1.400	3.026	2.756	2.675	2.341	1.866
	3.035	2.779	2.702	2.386	1.938
1.600	3.025	2.745	2.662	2.320	1.843
	3.034	2.769	2.690	2.367	1.922
1.800	3.024	2.735	2.649	2.300	1.829
	3.033	2.761	2.679	2.350	1.912
2.000	3.024	2.726	2.638	2.283	1.821
	3.034	2.753	2.669	2.336	1.906
		Σ_u			
1.000	0.099[−1]	0.718[−1]	0.103	0.307	0.701
	0.096[−1]	0.778[−1]	0.113	0.351	0.769
1.200	0.134[−1]	0.986[−1]	0.143	0.433	0.897
	0.130[−1]	0.107	0.157	0.492	0.964
1.400	0.174[−1]	0.136	0.199	0.616	1.109
	0.169[−1]	0.148	0.222	0.695	1.170
1.600	0.223[−1]	0.191	0.288	0.881	1.316
	0.218[−1]	0.211	0.323	0.988	1.369
1.800	0.284[−1]	0.283	0.441	1.230	1.498
	0.280[−1]	0.317	0.503	1.331	1.546
2.000	0.367[−1]	0.466	0.754	1.603	1.649
	0.366[−1]	0.540	0.876	1.682	1.693
		Π_u			
1.000	0.331[−2]	0.397[−1]	0.582[−1]	0.175	0.401
	0.322[−2]	0.444[−1]	0.662[−1]	0.208	0.466
1.200	0.371[−2]	0.467[−1]	0.686[−1]	0.204	0.441
	0.358[−2]	0.526[−1]	0.785[−1]	0.243	0.509
1.400	0.419[−2]	0.545[−1]	0.800[−1]	0.234	0.478
	0.402[−2]	0.618[−1]	0.922[−1]	0.280	0.548
1.600	0.475[−2]	0.630[−1]	0.924[−1]	0.265	0.512
	0.452[−2]	0.718[−1]	0.107	0.317	0.583
1.800	0.540[−2]	0.723[−1]	0.106	0.296	0.544
	0.513[−2]	0.829[−1]	0.123	0.356	0.615
2.000	0.613[−2]	0.822[−1]	0.120	0.327	0.572
	0.582[−2]	0.946[−1]	0.140	0.393	0.643

TABLE IV. Electron-H_2 cross sections (in a_0^2) for excitations $v_0,j_0 \rightarrow v,j$ at selected energies (in eV), as calculated with the BTAD (upper) and CP (lower) polarization potentials using the ANV method. (Corresponding results from LFCC calculations appear in Table II.) In the rows labeled ESE, exchange was included exactly, using the iterative static-exchange method (Ref. 34).

	$\sigma(a_0^2)$					
	0,0→0,0	0,0→0,2	0,0→1,0	0,0→1,2	0,0→2,0	0,0→2,2
			$E=0.7$ eV			
ANV (TFEGE)	47.825	1.555	0.156	0.127		
	43.316	1.846	0.202	0.169		
ANV (ESE)	42.754	1.458	0.145	0.110		
	39.938	1.673	0.183	0.138		
			$E=1.5$ eV			
ANV (TFEGE)	52.617	3.682	0.574	0.648	0.026	0.046
	51.773	4.556	0.762	0.865	0.041	0.071
ANV (ESE)	48.898	3.647	0.581	0.620	0.023	0.041
	49.143	4.377	0.750	0.789	0.034	0.058
			$E=3.5$ eV			
ANV (TFEGE)	51.058	6.119	0.670	0.924	0.050	0.073
	53.991	6.971	0.754	1.027	0.061	0.084
ANV (ESE)	50.974	6.534	0.720	0.954	0.052	0.075
	54.589	7.251	0.791	1.025	0.061	0.081
			$E=6.0$ eV			
ANV (TFEGE)	41.822	5.575	0.403	0.572	0.029	0.037
	45.212	5.827	0.409	0.562	0.030	0.036
ANV (ESE)	43.547	5.866	0.411	0.556	0.029	0.036
	47.196	5.991	0.412	0.532	0.030	0.033
			$E=10.0$ eV			
ANV (TFEGE)	29.946	4.099	0.203	0.264	0.012	0.015
	32.816	4.065	0.201	0.248	0.012	0.013
ANV (ESE)	32.068	4.112	0.196	0.235	0.012	0.013
	34.903	4.014	0.192	0.217	0.011	0.011

percent difference in $\sigma(0,0\rightarrow1,0)$ increases from 11% at 0.7 eV (near the threshold energy for this excitation, 0.516 eV) to 38% at 1.5 eV. Similarly, the difference in $\sigma(0,0\rightarrow1,2)$ (threshold energy is 0.599 eV) increases from 23% at 0.7 eV to 39% at 1.5 eV. These differences are manifestations of the differences between the CP and BTAD vibrational matrix elements shown in Fig. 2.

Differential cross sections at 1.5 eV, the energy at which the cross sections in Fig. 7 are most sensitive to the polarization potential, are shown in Fig. 8. At this energy (and at others below several eV) the CP and BTAD cross sections $\sigma(0,0\rightarrow1,0)$ exhibit differences of scale and of shape, suggesting that the two models yield different mixtures of partial waves in this cross section.

The differences between the CP and BTAD cross sections for excitations to $v=1$ are magnified in the $v_0=0\rightarrow v=2$ cross sections shown in Fig. 9. At 1.5 eV, for example, the difference in $\sigma(0,0\rightarrow2,0)$, the threshold for which is 1.002 eV, is 70% and that in $\sigma(0,0\rightarrow2,2)$, with threshold energy 1.042 eV, is 71%. The corresponding differential cross sections (not shown) manifest the *sensitivity* seen in the $v_0=0\rightarrow v=1$ cross sections of Fig. 8, but this sensitivity is more pronounced for $v=2$ than for $v=1$.

E. Discussion of theoretical results and comparison to experimental data

The low-energy results shown in Secs. IV B—IV C exhibit considerable sensitivity to the polarization potential used to calculate them. To indicate the importance of this sensitivity, we compare in Tables V and VI theoretical results for total (i.e., elastic plus rotational-excitation), momentum-transfer, pure rotational, and vibrational-excitation cross sections from the present BTAD and CP calculations with data from a variety of experiments. Low-scattering energies, at which the sensitivity to polarization is greatest, are emphasized.[40] An extensive discussion of our BTAD and experimental e-H_2 cross section data appears elsewhere.[41]

Examination of the results in Tables II and IV shows that the sensitivity of vibrational-excitation cross sections depends on other assumptions made in formulating the collision theory. For example, at energies below 3.0 eV, the difference between the BTAD and CP vibrational-excitation cross sections depends on the scattering theory used (LFCC or ANV) and on how exchange is represented (exactly or via the FEG model potential). Thus, at 1.5 eV, the difference between the BTAD and CP $\sigma(0,0\rightarrow2,0)$ is

TABLE V. Comparison of theoretical e-H_2 cross sections (in $\AA^2$) at selected energies (in eV) with experimental data. For each entry, the upper value was calculated with the BTAD polarization potential, allowing for the nuclear motion as described in Sec. IV. The value below this one (in parentheses) was calculated using the CP potential, also taking account of the nuclear motion. Results in square brackets, however, were calculated using the BTAD potential *in the rigid-rotator approximation* with the internuclear separation of H_2 fixed at its equilibrium value, $1.4a_0$. Total (tot), momentum transfer (MT), and pure rotational excitation $(0,0\rightarrow 0,2)$ cross sections are shown.

E (eV)	σ_{tot}^{theor} ($\AA^2$)	σ_{tot}^{expt} ($\AA^2$)[a]	σ_{MT}^{theor} ($\AA^2$)	σ_{MT}^{expt} ($\AA^2$)[b]	σ^{theor} ($\AA^2$) $(0,0\rightarrow 0,2)$	σ^{expt} ($\AA^2$) $(0,0\rightarrow 0,2)$[b]
0.047	8.026	8.234	8.786	9.10	0.018	0.018
	(6.841)		(7.565)		(0.020)	
	[6.812]		[8.736]		[0.016]	
0.08	8.642	8.79	9.688	10.0	0.060	0.060
	(7.436)		(8.448)		(0.061)	
	[7.384]		[9.596]		[0.055]	
0.10	8.925	9.19	10.122	10.5	0.074	0.074
	(7.718)		(8.886)		(0.075)	
	[7.651]		[10.008]		[0.067]	
0.20	9.924	10.05	11.743	12.0	0.124	0.120
	(8.743)		(10.567)		(0.131)	
	[8.618]		[11.535]		[0.110]	
0.50	11.596	11.62	14.646	14.7	0.279	0.278
	(10.651)		(13.850)		(0.317)	
	[10.347]		[14.207]		[0.239]	

[a]Ferch *et al.* (Ref. 43).
[b]Crompton *et al.* (Ref. 44).

70% when the LFCC method is used and 58% when the ANV method is used.

Other than the use of a model polarization potential, the central approximation in the present study is the FEG treatment of exchange effects. Some measure of the accuracy of our TFEGE potential can be gleaned from Table IV by comparing ANV inelastic cross sections from exact and model exchange calculations. Thus, at 0.07 eV, where the sensitivity to exchange is the greatest, the TFEGE introduces an error of 7% in $\sigma(0,0\rightarrow 1,0)$ and 11% in $\sigma(0,0\rightarrow 1,2)$. (The accuracy of the TFEGE seems little affected by whether the BTAD or CP potentials are used to model polarization.) Unfortunately, at present we do not know whether the same order of difference between exact and TFEGE cross sections would be found in a full rovibrational LFCC calculation; this question is currently under investigation in our group.

Of course, the ANV approximation introduces considerable error into these low-energy cross sections, as can be seen in Table IV. But even the measure of this error depends to some extent on the polarization potential. At 1.5 eV, for instance, the ANV $\sigma(0,0\rightarrow 2,2)$ differs from its LFCC counterpart by 318% if the BTAD potential is used and by 274% if the CP is used. This phenomenon is probably due to the sensitivity of the commutator of the nuclear Hamiltonian and the interaction potential to the polarization component of this potential; the accuracy of the AN approximation hinges on this commutator being

TABLE VI. Comparison of theoretical e-H_2 cross sections for the excitation $v_0=0\rightarrow v=1$ at selected energies (in eV) with data from swarm (S) and beam (B) experiments. These cross sections (in $\AA^2$) are summed over final rotational states j. For each entry, the upper (lower) cross sections was determined in LFCC calculations using the BTAD (CP) potential; the CP results are in parentheses.

Energy (eV)	σ^{theor}	$\sigma_S^{expt\,a}$	$\sigma_B^{expt\,b}$
0.60	0.008	0.009	0.0172
	(0.014)		
0.70	0.023	0.020	0.032
	(0.026)		
1.00	0.089	0.064	0.094
	(0.116)		
1.50	0.254	0.200	0.246
	(0.351)		
3.50	0.464		0.490
	(0.529)		
4.50	0.394		0.391
	(0.420)		

[a]Crompton *et al.* (Ref. 45).
[b]Ehrhardt *et al.* (Ref. 46).

negligible in the Schrödinger equation in the body frame.[42]

V. CONCLUSIONS

The sensitivity of e-H_2 vibrational-excitation cross sections to the choice of model polarization potential is of some concern. To be sure, elements of both models investigated in this study are somewhat *ad hoc,* but each incorporates the essential physics of polarization at long and intermediate range and of correlation at short range, and each is based on a reasonable theoretical foundation. This sensitivity may imply that, at least for vibrational excitation of H_2, considerable precision in one's model polarization potential is necessary if accurate cross sections are to be obtained. At the very least, these findings emphasize the need for more rigorous calculations of *ab initio* eigenphase sums (for a range of internuclear separations) and of vibrational-excitation cross sections—say, in an optical-potential formulation. The results in Table IV reemphasize the importance in the calculation of these cross sections of accurately representing the dynamical "coupling" of the motion of the scattering electron and that of the nuclei.

The comparison of theoretical and experimental cross sections in Tables V and VI suggests that for low-energy vibrational excitation of H_2, the BTAD may be a more accurate approximate representation of polarization than the CP potential. Considering the issues discussed in Sec. IV E, however, we think it would be rash to generalize this finding to any other molecule. In our group an investigation of this matter for e-N_2 scattering is nearing completion; but it is also important that such a study be pursued for electron scattering from a strongly polar molecule, such as HCl, where the nature of the electron-molecule interaction is drastically different from that in e-H_2.

The findings of this study notwithstanding, we consider the CP potential a very promising model of polarization effects. The importance of accurately taking account of the vibrational motion of the nuclei in calculations of inelastic electron-molecule cross sections and the ease with which the CP potential can be evaluated argue strongly for its consideration in the future, particularly when complicated, technologically important systems, such as large, many-electron polyatomic molecules, clusters, and surfaces, are of interest.

ACKNOWLEDGMENTS

The authors are grateful to Dr. Andrew N. Feldt, Dr. Nely Padial, and Dr. Thomas L. Gibson for useful conversations and encouragement throughout this research. We would also like to thank Dr. David W. Norcross for generously giving of his time, insight, and incisive criticism to the improvement of this manuscript. This work was supported by Grant No. PHY-8505438 from the National Science Foundation.

[1]N. F. Lane, Rev. Mod. Phys. **52**,29 (1980).

[2]M. A. Morrison, Aust. J. Phys. **36**, 239 (1983).

[3]L. Castillejo, I. C. Percival, and M. J. Seaton, Proc. R. Soc. London, Ser. A **254**, 259 (1960).

[4]M. A. Morrison and P. J. Hay, Phys. Rev. A **20**, 740 (1979).

[5]R. A. Eades, D. A. Dixon, and D. G. Truhlar, J. Phys. B **15**, 2265 (1982), and references therein.

[6]N. F. Lane and R. J. W. Henry, Phys. Rev. **173**, 183 (1968); S. Hara, J. Phys. Soc. Jpn. **27**, 1262 (1969).

[7]T. L. Gibson and M. A. Morrison, Phys. Rev. A **29**, 2497 (1984); J. Phys. B **15**, L221 (1982). For details see T. L. Gibson, Ph.D. thesis, University of Oklahoma, 1982.

[8]The Pople-Schofield method of treating polarization has been used by A. Jain and D. G. Thompson, J. Phys. B **15**, L631 (1982).

[9]For recent applications of the polarized-orbital method to electron-molecule scattering, see K. Onda and D. G. Truhlar, Phys. Rev. A **22**, 86 (1980); K. Onda and A. Temkin, *ibid.* **28**, 621 (1983).

[10]For treatments of polarization based on pseudostates see, for example, B. I. Schneider, Chem. Phys. Lett. **51**, 578 (1977); R. K. Nesbet, C. J. Noble, L. A. Morgan, and C. A. Weatherford, J. Phys. B **17**, L891 (1984).

[11]A second-order optical potential has been used to treat polarization by A. Klonover and U. Kaldor, Chem. Phys. Lett. **51**, 321 (1977); J. Phys. B **12**, 3797 (1979), and references therein. For other optical-potential calculations of electron-molecule scattering, see B. I. Schneider and L. A. Collins, J. Phys. B **15**, L335 (1982); Phys. Rev. A **27**, 2847 (1983); **28**, 166 (1983); **30**, 95 (1984); G. Staszewska, D. W. Schwenke, and D. G. Truhlar, J. Chem. Phys. **81**, 335 (1984); P. G. Burke, C. J. Noble, and S. Salvini, J. Phys. B **16**, L113 (1984); and L. A. Morgan and C. J. Noble, *ibid.* **17**, L369 (1984).

[12]A many-body optical potential has been applied to resonant e-N_2 scattering by M. Berman, O. Walter, and L. S. Cederbaum, Phys. Rev. Lett. **50**, 1979 (1983).

[13]The multichannel Schwinger method has been used to treat polarization by K. Takatsuka and V. McKoy, Phys. Rev. A **24**, 2473 (1981); T. L. Gibson, M. A. P. Lima, K. Takatsuka, and V. McKoy, *ibid.* **30**, 3005 (1984).

[14]M. Berman and U. Kaldor, J. Phys. B **14**, 3993 (1981); Chem. Phys. Lett. **79**, 489 (1981).

[15]J. K. O'Connell and N. F. Lane, Phys. Rev. A **27**, 1893 (1983).

[16]N. T. Padial and D. W. Norcross, Phys. Rev. A **29**, 1742 (1984); **29**, 1590 (1984); N. T. Padial, *ibid.* **32**, 1379 (1985).

[17]A. Jain and D. W. Norcross, Phys. Rev. A **32**, 134 (1985); J. Chem. Phys. **84**, 739 (1986). For an application of the CP potential to intermediate-energy electron-molecule scattering, see P. K. Bhattacharyya, D. K. Syamal, and B. C. Saha, Phys. Rev. A **32**, 854 (1985).

[18]For a discussion of corrections to the adiabatic polarization potential for *electron-atom* systems, see, for example, J. Callaway, R. W. LaBahn, R. T. Pu, and W. M. Duxler, Phys. Rev. **168**, 12 (1968); C. J. Kleinman, Y. Hahn, and L. Spruch, *ibid.* **165**, 53 (1968); A. Dalgarno, G. W. F. Drake, and G. A. Victor, *ibid.* **176**, 194 (1968); A. Dalgarno and P. Shorer, Phys.

Rev. A 20, 1307 (1979); and D. W. Norcross, *ibid.* 28, 3095 (1983).

[19]See, for example, M. A. Morrison, N. F. Lane, and L. A. Collins, Phys. Rev. A 15, 2186 (1977); N. T. Padial, D. W. Norcross, and L. A. Collins, *ibid.* 27, 141 (1983). See also F. A. Gianturco and D. G. Thompson, J. Phys. B 13, 613 (1980).

[20]There are a variety of ways to determine the cutoff parameter. See, for example, A. Jain and D. G. Thompson, J. Phys. B 16, 2593 (1983); 16, 3077 (1983); 17, 443 (1983); A. Jain and S. S. Tayal, *ibid.* 17, L37 (1984); A. Jain, J. Chem. Phys. 81, 724 (1984); and N. Abusalbi, R. A. Eades, T. Nam, D. Thirumalai, D. A. Dixon, and D. G. Truhlar, *ibid.* 78, 1213 (1983).

[21]A. Temkin, Phys. Rev. 107, 1004 (1957).

[22]M. A. Morrison, A. N. Feldt, and D. Austin, Phys. Rev. A 29, 2518 (1984).

[23]M. A. Morrison, A. N. Feldt, and B. C. Saha, Phys. Rev. A 30, 2811 (1984).

[24]T. L. Gibson, B. C. Saha, and M. A. Morrison, Bull. Am. Phys. Soc. 30, 881 (1985).

[25]For recent reviews of vibrational excitation in electron-molecule scattering see D. G. Thompson, Adv. At. Mol. Phys. 19, 309 (1983), and A. Herzenberg, in *Electron-Molecule Collisions,* edited by I. Shimamura and K. Takayanagi (Plenum, New York, 1984), p. 191. Valuable reviews of experimental data on this scattering process can be found in G. J. Schulz, in *Principles of Laser Plasmas,* edited by G. Bekite (Wiley, New York, 1976), Chap. 2, and in the comprehensive review by S. Trajmar, D. F. Register, and A. Chutjian, Phys. Rep. 97, 219 (1983).

[26]Earlier studies of vibrational excitation in e-H_2 scattering include R. J. W. Henry and E. S. Chang, Phys. Rev. A 5, 276 (1972); E. S. Chang, Phys. Rev. Lett. 33, 1644 (1974); C. Mündel, M. Berman, and W. Domcke, Phys. Rev. A 32, 181 (1985).

[27]J. P. Perdew and A. Zunger, Phys. Rev. B 23, 5048 (1981).

[28]M. A. Morrison, Comput. Phys. Commun. 21, 63 (1980); L. A. Collins, D. W. Norcross, and G. B. Schmid, *ibid.* 21, 79 (1980).

[29]If these functions intersect at more than one point, the *smallest* such point is taken as the joining radius, for that point will be nearest the boundary of the target charge distribution. See Ref. 15 for discussion of this point.

[30]J. W. Moskowitz and L. C. Snyder, in *Methods of Electronic Structure Theory,* edited by H. F. Schaeffer III (Plenum, New York, 1977), p. 387.

[31]S. Huzinaga, J. Chem. Phys. 43, 1293 (1965).

[32]M. A. Morrison, A. N. Feldt, and B. C. Saha (unpublished).

[33]D. M. Chase, Phys. Rev. 104, 838 (1956); S. Hara, J. Phys. Soc. Jpn. 27, 1593 (1969); A. Temkin and K. V. Vasavada, Phys. Rev. 160, 109 (1967); E. S. Chang and A. Temkin, Phys. Rev. Lett. 23, 399 (1969); F. H. M. Faisal and A. Temkin, *ibid.* 28, 203 (1972).

[34]L. A. Collins, W. D. Robb, and M. A. Morrison, Phys. Rev. A 21, 488 (1980).

[35]A. M. Arthurs and A. Dalgarno, Proc. R. Soc. London, Ser. A 256, 540 (1960). For application of this method to vibrational excitation, see R. J. W. Henry, Phys. Rev. A 2, 1349 (1970).

[36]See M. A. Morrison and L. A. Collins, Phys. Rev. A 17, 918 (1978); and T. L. Gibson and M. A. Morrison, J. Phys. B 14, 717 (1981), and references therein.

[37]M. A. Morrison and L. A. Collins, Phys. Rev. A 23, 127 (1981).

[38]Elastic scattering at energies below several eV is dominated by s-wave S-matrix elements, and the adequacy of $V_{\rm pol}^{\rm CP}(r_e,R)$ for these cross sections is mirrored in the (s-wave-dominated) fixed-nuclei Σ_g eigenphase sum. The CP potential produces Σ_g eigenphase sums that, as a function of internuclear separation, closely parallel those obtained using the BTAD potential.

[39]For example, the contribution from p-wave T-matrix elements to $\sigma(0,0\rightarrow 1,0)$ is greater than 80%, and to $\sigma(0,0\rightarrow 1,2)$ a whopping 99%. The next most important contributors to these cross sections come from the Π_u and then the Σ_g symmetries.

[40]At energies above a few eV, the accuracy of the theoretical inelastic cross sections becomes somewhat questionable; with increasing energy, symmetries other than Σ_u begin to contribute significantly to these cross sections, and exchange is less well represented in these symmetries by our TFEGE potential than in the tuning symmetry, Σ_u.

[41]R. W. Crompton and M. A. Morrison, in *Swarm Studies and Inelastic Electron-Molecule Collisions,* edited by A. Chutjian, V. McKoy, L. C. Pitchford, and S. Trajmar (Springer-Verlag, Berlin, 1986); and M. A. Morrison, R. W. Crompton, B. C. Saha, and Z. Petrovic, Aust. J. Phys. (to be published).

[42]E. S. Chang and U. Fano, Phys. Rev. A 6, 173 (1972).

[43]J. Ferch, W. Raith, and K. Schröder, J. Phys. B 13, 1481 (1980).

[44]R. W. Crompton, D. K. Gibson, and A. I. McIntosh, Aust. J. Phys. 22, 715 (1969); R. W. Crompton (private communication). See also S. J. Buckman and A. V. Phelps, Joint Institute for Laboratory Astrophysics Data Center Report No. 27, 1985 (unpublished).

[45]R. W. Crompton, D. K. Gibson, and A. G. Robertson, Phys. Rev. A 2, 1386 (1970); D. K. Gibson, Aust. J. Phys. 23, 683 (1970); R. W. Crompton (private communication).

[46]H. Ehrhardt, L. Langhans, F. Linder, and H. S. Taylor, Phys. Rev. 173, 222 (1968); F. Linder and Z. Schmidt, Z. Naturforsch. 26a, 1603 (1981).